ALE AND FLUID-STRUCTURE INTERACTION IN LS-DYNA

M'hamed Souli
USTL
Université des Sciences de Lille et Technologie
Laboratoire de Mécanique de Lille, Villeneuve d'Ascq, France
e-mail: Mhamed.Souli@univ-lille1.fr

ABSTRACT

A new Eulerian-Lagrangian coupling algorithm and improved multi-material ALE-capabilities have made LS-DYNA an efficient tool for analyzing large deformation processes, such as bird strike events and forging operations. This paper contains two example problems that illustrate the current features of the code.

INTRODUCTION

Numerical problems due to element distortions limit the applicability of a Lagrangian description of motion when modeling large deformation processes.

An alternative technique is the multi-material Eulerian formulation. It is a method where the material flows through a mesh that is completely fixed in space and where each element is allowed to contain a mixture of different materials. The method completely avoids element distortions and it can, through an Eulerian-Lagrangian coupling algorithm, be combined with a Lagrangian description of motion for parts of the model.

The Eulerian formulation is not free from numerical problems. There are dissipation and dispersion problems associated with the flux of mass between elements. In addition, many elements might be needed for the Eulerian mesh to enclose the whole space where the material will be located during the simulated event.

This is where the multi-material arbitrary Lagrangian-Eulerian (ALE) formulation has its advantages. By translating, rotating and deforming the multi-material mesh in a controlled way, the mass flux between elements can be minimized and the mesh size can be kept smaller than in an Eulerian model. The idea is visualized in Figure 1.

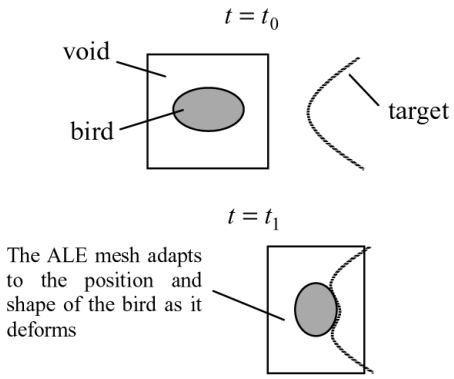

Figure 1. Moving ALE-mesh in impact simulation

CONTROLLED ALE-MESH MOTION

In LS-DYNA, the ALE-mesh motion can be defined with four different methods:

1. Classical mesh smoothing
2. Motion following pre-defined load curves
3. Automatic translation, rotation and stretching of elements in order to adapt to the current location of the material inside the mesh
4. Automatically translate and rotate the mesh, following a coordinate system defined by three arbitrary nodes in the model

The classical mesh smoothing algorithms [Hallquist et al. 1998] and the automatic translation following three arbitrary nodes are not discussed in this paper.

Pre-Defined Load Curve Motion

The load curve driven motion needs a set of twelve load curves. The velocity of a node coordinate $(x,y,z)_i$ is defined as

$$\begin{Bmatrix} \dot{x} \\ \dot{y} \\ \dot{z} \end{Bmatrix}_i = \begin{Bmatrix} f_1 \\ f_2 \\ f_3 \end{Bmatrix} + \begin{bmatrix} f_4 & f_5 & f_6 \\ f_7 & f_8 & f_9 \\ f_{10} & f_{11} & f_{12} \end{bmatrix} \begin{Bmatrix} x \\ y \\ z \end{Bmatrix}_i ,$$

where $f_i(t)$, i=[1,12] are the user defined load curves. This prescribed node motion allows rigid body translations, rotations and mesh shrinking/expansion.

Automatic Motion

The automatic motion is preferable if one does not know ahead of time how the material is going to move.

As a special case the mesh is given a rigid body translation where the node velocity, $\dot{\mathbf{x}}_c$, is defined as

$$\dot{\mathbf{x}}_c = \begin{Bmatrix} \dot{x}_c \\ \dot{y}_c \\ \dot{z}_c \end{Bmatrix} = \sum_{i=1}^{nn} m_i \begin{Bmatrix} u \\ v \\ w \end{Bmatrix}_i \Big/ \sum_{i=1}^{nn} m_i \ .$$

m_i , i=[1, nn] are the nodal masses in the ALE-mesh and $(u,v,w)_i$ are the nodal mass flow velocities in the x, y and z-directions, respectively.

The default is to allow the mesh to expand and shrink in order to better follow the material flow. For this, a spatially linear velocity field is defined. It is required to know the center of gravity, $\mathbf{x}_c$, of the ALE-mesh.

$$\mathbf{x}_c = \begin{Bmatrix} x_c \\ y_c \\ z_c \end{Bmatrix} = \sum_{i=1}^{nn} m_i \begin{Bmatrix} x \\ y \\ z \end{Bmatrix}_i \Big/ \sum_{i=1}^{nn} m_i$$

Looking at one Cartesian direction at the time, measures of the average mesh expansion velocities are defined as

$$\dot{x}' = \frac{\sum_{i=1}^{nn} (x_i - x_c)(u_i - \dot{x}_c) m_i}{\sum_{i=1}^{nn} (x_i - x_c)^2 m_i}$$

$$\dot{y}' = \frac{\sum_{i=1}^{nn} (y_i - y_c)(v_i - \dot{y}_c) m_i}{\sum_{i=1}^{nn} (y_i - y_c)^2 m_i}$$

$$\dot{z}' = \frac{\sum_{i=1}^{nn} (z_i - z_c)(w_i - \dot{z}_c) m_i}{\sum_{i=1}^{nn} (z_i - z_c)^2 m_i}$$

The angular velocities are estimated as

$$\omega_x = \frac{\sum_{i=1}^{nn}[(y_i - y_c)(w_i - \dot{z}_c) - (z_i - z_c)(v_i - \dot{y}_c)]m_i}{\sum_{i=1}^{nn} r_i^2 m_i}$$

$$\omega_y = \frac{\sum_{i=1}^{nn}[(z_i - z_c)(u_i - \dot{x}_c) - (x_i - x_c)(u_i - \dot{x}_c)]m_i}{\sum_{i=1}^{nn} r_i^2 m_i}$$

$$\omega_z = \frac{\sum_{i=1}^{nn}[(x_i - x_c)(v_i - \dot{y}_c) - (y_i - y_c)(v_i - \dot{y}_c)]m_i}{\sum_{i=1}^{nn} r_i^2 m_i}$$

r_i is the distance between $\mathbf{x}_i$ and $\boldsymbol{x}_c$. From this, the node velocity at a coordinate $(x,y,z)_i$ is defined as

$$\dot{\mathbf{x}}_i = \begin{Bmatrix} \dot{x}_c \\ \dot{y}_c \\ \dot{z}_c \end{Bmatrix} + \begin{bmatrix} \dot{x}' & -\omega_z & \omega_y \\ \omega_z & \dot{y}' & -\omega_x \\ -\omega_y & \omega_x & \dot{z}' \end{bmatrix} \begin{Bmatrix} x_i - x_c \\ y_i - y_c \\ z_i - z_c \end{Bmatrix}$$

That is, the velocity at the center of gravity equals $\dot{\mathbf{x}}_c$.

FLUID-STRUCTURE COUPLING

A new Eulerian-Lagrangian coupling algorithm was implemented in the 960 version of LS-DYNA. It is penalty-based and it is defined to preserve the total energy of the system as well as possible. The old constraint based methods consume some kinetic energy, which is a problem in many impact applications.

The basic idea of the penalty formulation is to track the relative displacements between the coupled Lagrangian nodes and the fluid. The coupling forces are defined to be proportional to these displacements.

The theory is not included in this paper. However, the first application example compares the energy conservation in the penalty-based method with a classical constraint based one.

BIRD STRIKE SIMULATION

The usefulness of the moving mesh technique is displayed in a small model of an elastic ideally plastic bird hitting a rigid wall. Figure 2 shows the geometry (plane strain). The properties of the bird material are

$$\rho = 78.0\ kg/m^3$$
$$E = 1.0 \cdot 10^5\ Pa$$
$$\nu = 0.3$$
$$\sigma_y = 1.0 \cdot 10^3\ Pa$$

ρ is the density, E and ν are the Young's modulus and the Poisson's ratio, respectively, and σ_y is the von Mises yield stress.

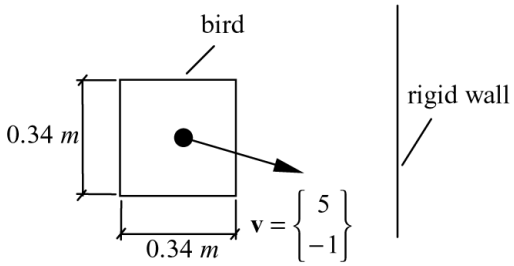

Figure 2. Square bird impacting rigid wall

The problem is solved with two different methods, one applying a moving ALE-mesh technique for the multi-material bird and one is purely Eulerian.

Multi-Material ALE Model

Here the bird is modeled enclosed in a layer of void (vacuum). The mesh follows the bird and expands with the automatic mesh moving technique described above. The mesh and the deformations of the bird are shown in Figures 3 and 4. Energy curves are presented in Figure 5. The decay of the total energy is due to dissipation when fluxing solution variables between adjacent elements.

Multi-Material Eulerian Model

In the multi-material Eulerian approach a larger region of void needs to be modeled, see Figure 4. Since the elements are fixed in space the relative motion between bird and mesh is larger than with the ALE-formulation. The geometry of the bird is distorted as it moves through the mesh and there is substantial energy dissipation, see Figures 4 and 5.

Constraint Based Coupling

To show the importance of energy preservation in the coupling, the problem is also solved with a constraint based Eulerian-Lagrangian coupling algorithm. The multi-material ALE- model, see Figure 3, is used. The energy preservation curve is shown in Figure 5.

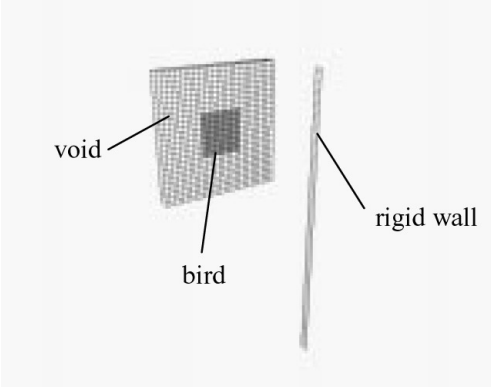

Figure 3. Multi-material ALE-model

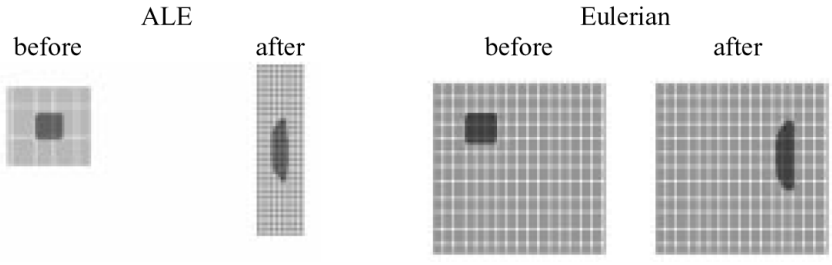

Figure 4. Multi-material bird before and after impact

FORGING PROBLEM

A small forging problem was solved with the purpose of comparing the results from the multi-material approach with those obtained with a purely Lagrangian formulation. Due to element distortions, the Lagrangian model failed in running to completion and the results are compared at a relatively early stage of the process.

Figure 6 shows the Lagrangian and Eulerian models. The work-piece is elastic, ideally plastic.

Figure 7 shows the cross section of the Eulerian work-piece at different stages of the process. The effective plastic strain distribution along a line cutting through the work-piece is presented in Figure 8.

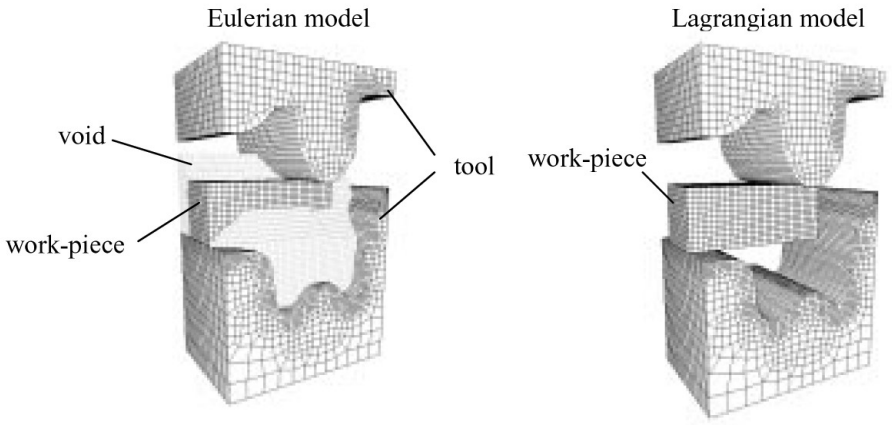

Figure 6. Eulerian and Lagrangian forging models

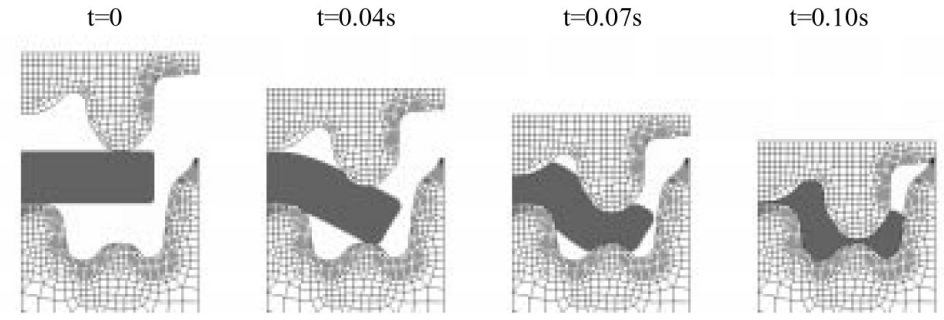

Figure 7. Cross section of Eulerian work-piece at different stages of the process

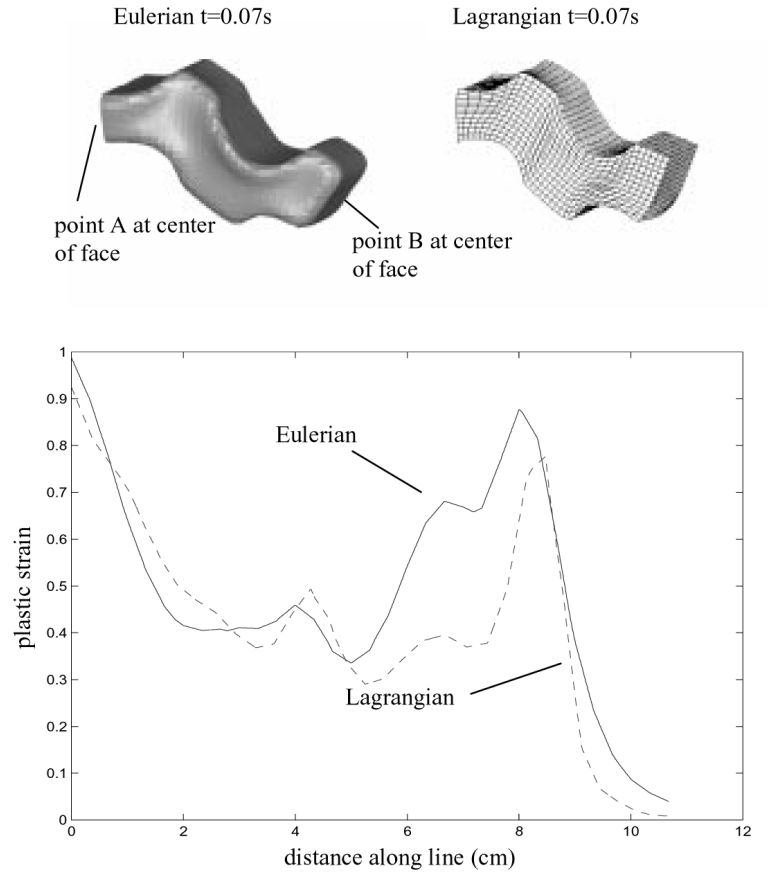

Figure 8. Effective plastic strain level at time 0.07s along a straight line between material point A and B

REFERENCE

HALLQUIST, J.O. (1998), LS-DYNA *Theoretical Manual*, Livermore Software Technology Corporation, Livermore